

NASA/CR-99-

206470

Final  
11-15-97

OCIT

125925

# AN INVESTIGATION INTO QUANTIFYING $\mu\text{G}$ CHANGES IN A GRAVITATIONAL FIELD OF 1G

UAH final report for  
NASA Contract No. NAS8-97095 Task H-28436D

"OPTICAL MEASUREMENTS OF ACCELERATION FIELDS"

Submitted to:  
George C. Marshall Space Flight Center  
National Aeronautics and Space Administration  
Marshall Space Flight Center, Alabama 35812

Prepared by: Richard R. Gauthier, M.S.  
Under the direction of: John A. Gilbert, Ph.D.

Consortium for Holography, Applied Mechanics and Photonics  
University of Alabama in Huntsville  
Huntsville, Alabama, 35899  
(205) 890-6029 X391

November 1997

## TABLE OF CONTENTS

Description	Page
COVER PAGE .....	i
TABLE OF CONTENTS .....	ii
INTRODUCTION .....	1
BACKGROUND .....	1
OBJECTIVE .....	2
FIELD MEASUREMENT .....	2
DEVICE REQUIREMENTS .....	3
DESIGN OF THE TRANSVERSELY SUSPENDED ACCELEROMETER (TSA) .....	4
DEVELOPMENT OF THE TSA .....	5
PROTOTYPE FABRICATION .....	7
CALIBRATION .....	7
MAGNETIC EFFECTS .....	8
CONCLUSIONS .....	9
REFERENCES .....	9
ACKNOWLEDGEMENTS .....	10
FIGURES .....	11
APPENDIX 1. SENSOR DESIGN DATA .....	16
APPENDIX 2. SENSOR CALIBRATION DATA AND SPECIFICATIONS .....	17

## INTRODUCTION

This project called for the development of an accelerometer designed to be used in conjunction with gravity shielding experiments. The device had to measure local gravitational changes on the order of a few micro-G's ( $\mu\text{G}$ )<sup>1</sup> with a spatial resolution greater than one measurement per ten (10) square centimeters. Measurements had to be made at a minimum rate of two (2) per second. Tasks included the design, development and demonstration of a prototype. The deliverable consisted of three copies of this final report.

The study resulted in the development of a Transversely Suspended Accelerometer (TSA) which met all of the technical specifications (see Appendices 1 and 2 for details). Different generations of the device were demonstrated to NASA/MSFC personnel as they were developed. The final prototype (see Fig. 2 for a schematic) is available for further demonstration and future use.

The study draws attention to the fact that the magnetic fields required to produce gravitational shielding may result in apparent decreases in the weights of suspended objects on the order of those attributed to the effect itself. This observation reinforces the need to quantify the influences of the magnetic field on any measurement device used to study gravitational shielding. This task was accomplished for the TSA (the plot labeled as Paramagnetically Treated in Fig. 3 shows the result).

## BACKGROUND

Several years ago, the possibility of a new phenomenon called gravitational shielding (GS) was reported by Podkletnov and Nieminen [1]. They claimed that material objects placed above a superconducting apparatus experienced a decrease in weight on the order of one percent the normal weight. The phenomenon was observed while spinning a large superconducting disk using high frequency magnetic fields. The disk, cooled to a temperature below 77 K, levitated in a static magnetic field according to the Meissner effect.

Although the potential applications for this phenomenon are staggering, studies involving GS still remain in the embryonic stages of development. There has been some experimental verification of the effect [2], but many questions remain concerning how it is produced, and whether GS actually corresponds to a local modification of the earth's gravitational field. There is a critical need to obtain a precise knowledge of the experimental conditions under which the effect is observed.

A limited amount of theoretical work has been published [3-5] which suggests different possible mechanisms for GS. It would be possible to discriminate between these theories if accurate data

---

<sup>1</sup> The unit G is a nondimensional quantity which provides a measure of acceleration when the quantity is multiplied by the local gravitational acceleration,  $g = 9.81 \text{ m/s}^2$ .

could be acquired regarding functionality of the observable parameters. It would be very important, for example, to measure the spatial dependence of the effect in a plane above the disk, the vertical positional dependence, the directional dependence (including a possible effect at the sides of the disk), etcetera. A suitably designed gravimeter/accelerometer would help to meet these objectives.

## **OBJECTIVE**

The objective of this research was to develop a new device, based on optical metrology, specifically designed to quantify modifications of the local gravitational field in the vicinity of the experimental cryostat apparatus used to produce gravitational shielding (GS). Several preliminary investigations were performed during the contractual period which resulted in the production of a Transversely Suspended Accelerometer (TSA) having several advantageous features.

This report presents the design strategy, fabrication, calibration and testing of the TSA. The device is currently at the stage where it can be used to corroborate or augment existing theories and/or measurements pertaining to GS.

## **FIELD MEASUREMENT**

In order to design an accurate measurement device, the characteristics of the measurand must be known as exactly as possible. This was somewhat difficult in the case of GS, since a variety of physical principles could be involved in the expected weight decrease. Some assumptions were therefore necessary as a starting point for the design.

It was assumed that the measurand is indeed a change in the gravitational field, and that according to the reported effect, conditions of dynamic equilibrium result in an unvarying DC decrease in the magnitude of that field on the order of a percent, or, 10 milli-G's (mG). Therefore, the limit of sensitivity and precision for the measurement should be at least several hundred times smaller, or, on the order of tens of  $\mu\text{G}$ 's.

Rigorous consideration of the field requires a distinguishment (in the weak field approximation) of the gravitoelectric components; as opposed to the gravitomagnetic components which may also exist and possibly play a role in the GS effect. Although both gravitomagnetic and gravitoelectric components were considered, only the latter (customary field) was targeted for measurement.

Other theoretical considerations revealed that it was possible to experimentally observe effects of both the field itself and a non-zero field gradient. Although studies using a gradient-sensitive device may be worthwhile, in order to avoid combined effects, attempts were made to minimize the influence of the field gradient in the device itself. However, by spatial mapping with

sufficient resolution, field gradients can be determined.

Under these assumptions, the metrology of the field necessitates using a test mass suspended in static equilibrium. A knowledge of the field is acquired by measuring the displacement of the mass. Therefore, the design was based on a mechanical system (i.e. suspended mass), convolved with an optical system for measuring the displacement. Optical methods were chosen because they offer extremely high precision with minimal electromagnetic interference. A gravimeter of this type is essentially an accelerometer and the two terms can be used synonymously.

## DEVICE REQUIREMENTS

The preliminary design of the accelerometer focussed on the development of the sensor, with priority given to sensitivity, size, and magnetic considerations. At first, it was thought that an interferometric system would be necessary to achieve the sensitivity specified as part of the design requirements. Assuming that this would be the case, it had to be decided whether to operate the interferometer at a quadrature-biased point, or to utilize fringe counting, both of which required additional complexity. Before that decision had to be made, however, it was realized that a more simple diffraction-limited image positioning device could be developed which had interferometric sensitivity. It was envisioned that a point source located on the test mass would be magnified and imaged with a minimum feature size corresponding to the order of the wavelength of light used.

It was desirable to keep the physical size of the sensor as small as possible so that the highest spatial resolution could be obtained. Since the space surrounding the GS experiment could be limited, plans called for separating the measurement system into three different sections. The first section consisted of a laser source, optics, and fiber coupling. The second section was comprised of an opto-mechanical system forming a gravitational sensor with minimal complexity and size. The third section included a link (either free-space or fiber-optic) which routed the optical signal from the sensor to the remotely located hardware and electronics which provided display and/or computer interfacing. It was envisioned that the sensor would have to be customized; off-the-shelf components would be used wherever possible.

The sensitivity of the device was estimated by analyzing the mechanical system. To this end, an effective spring constant,  $k_{eff}$ , can be defined as,

$$F = k_{eff} y \tag{1}$$

where  $F$  is the applied force and  $y$  is the displacement measured from the initial position. For operation in 1 G, the equation,

$$m g = k_{eff} y_0 \tag{2}$$

gives the initial displacement,  $y_0$ , of the suspended mass,  $m$ . Assuming that a  $\delta g$  produces a corresponding  $\delta y$ , the sensitivity is given by,

$$\frac{\delta g}{g} = \frac{\delta y}{y_0} \quad (3)$$

Equation (3) reveals that for linear systems, the sensitivity is essentially determined by the initial displacement; which for a resolution approaching  $\mu\text{G}$ 's and a wavelength of 633 nm, implies that the initial stretch or displacement of the system must approach tens of centimeters.

### DESIGN OF THE TRANSVERSELY SUSPENDED ACCELEROMETER (TSA)

It was determined that a good design could be constructed by suspending a test mass on a horizontal length of optical fiber. As illustrated in Fig. 1, the end of the fiber would be imaged with simple optics at a remote viewing plane to determine the displacement. The device was subsequently referred to as a Transversely Suspended Accelerometer (TSA).

The design for the TSA capitalizes on the mechanical properties of the fiber; glass has excellent elastic characteristics and a low temperature coefficient. The accelerometer has the advantages that it can be made quite small, it offers two-axis operation, and can be made very sensitive by allowing a large initial deflection. In contrast to an interferometer, optical measurements are made independent of light intensity and polarization.

The mechanical response of the TSA was determined by solving a point-load beam deflection problem. For a cantilever beam of length  $l$  and the axis system shown in Fig. 1,

$$y = \frac{-F z^2}{6 E I} (3l - z) \quad (4)$$

In formulating Eq. (4), the load  $F$  is applied along the negative  $y$  direction at a distance  $z$  from the fixed end;  $E$  is the elastic modulus and  $I$  is the area moment of inertia measured around a centroidal axis perpendicular to  $F$ .

Assuming that a mass  $m$  is attached to the free end of the optical fiber, the magnitude of the initial deflection is determined, by setting  $z = l$  and dropping the minus sign, as

$$y_0 = \frac{m g l^3}{3 E I} \quad (5)$$

where, for an optical fiber of diameter  $d$ ,  $I = \pi d^4/64$ . Changes in the deflection are then found from,

$$\delta y = \delta g \frac{m l^3}{3 E I} . \quad (6)$$

Equation (6) can be used to establish the product  $ml^3$  by choosing the full possible range of measured  $\delta g$  and using the effective lens aperture for  $\delta y$ . The resolution is determined from the optical properties as explained later in the section labeled Prototype Fabrication. The mass and fiber length can then be selected and the necessary initial deflection calculated.

The responsivity of the TSA,

$$R = \frac{\delta G}{\delta y'} = \frac{\delta g}{g \delta y'} \quad (7)$$

can be used to convert displacements of  $\delta y'$  in the image plane to  $\mu G$ 's. This quantity is determined in terms of the effective spring constant and the effective mass, and these parameters can be measured experimentally to calibrate the device. For a magnification  $M$ ,  $\delta y' = M\delta y$ , and

$$R = \frac{k_{eff}}{g m_{eff}} \frac{1}{M} . \quad (8)$$

Thus, to convert to  $R$  for a distance  $s$  measured along  $z$  (other than 1 m from the imaging lens),  $R(z) = R/s$ .

## DEVELOPMENT OF THE TSA

A simple working model of the TSA was fabricated and put into a test situation, which provided insight for improvements. A second generation prototype was subsequently developed with emphasis placed on the experimental environment anticipated during GS testing.

In order to achieve the maximum sensitivity possible, the end of the fiber was tapered down to provide a point-source image, as opposed to the untapered 4 micron fiber core of the single-mode fiber selected for the design. In this case, the image in the viewing plane became an airy ring pattern with a small center spot. The spot size (FWHM),  $ss$ , is determined by the diffraction limit,

$$ss = \frac{1.22 \lambda f}{a} \quad (9)$$

where  $\lambda$  is the wavelength,  $f$  is the focal distance of the transfer lens and  $a$  is the diameter of the aperture.

Tapering the fiber end was found experimentally to provide a central image 6.05 times smaller than an untapered end. The rated resolution is chosen as 0.2 times this spot size, although low-noise spot intensity measurement and analysis could allow about an order of magnitude greater precision.

Another improvement was made in the overall size of the device by pre-forming the fiber. This was done by heating and shaping the fiber segment according to the opposite of the deflection curve determined by beam bending:

$$y(z) = c z^2 (3l - z) \quad (10)$$

where  $c = mg/6EI$ . Thus when the mass was placed onto the fiber, the fiber moved to a straight line geometry, allowing the sensitive portion of the accelerometer to be encapsulated in a very small straight tube.

First device tests revealed that the mass used (lucite) responded by mG's to a small permanent magnet. This observation was considered important, since counter-arguments to the gravity reduction reported in the literature involved parameters such as air pressure, electric fields, temperature, and magnetic effects. The latter may deserve the most attention, since the experimental arrangements used to demonstrate GS typically require strong magnetic fields up to several Tesla.

In their original experiments, Podkletnov and his colleagues suspended different objects (glass, wood, plastic, metals...) above their apparatus, and used a sensitive balance to measure the weights of the objects. Although all of the above mentioned materials are diamagnetic (most, but not all metals), it does not appear that this magnetic interaction was taken into account.

As demonstrated later in the section labeled Magnetic Effects, magnetic fields of even 0.3 T can possess gradients high enough to produce a force on a "non-magnetic" material equivalent to several mG's: close to a percent of the material's weight. Furthermore, the apparent weight will *decrease* for diamagnetic objects suspended above the field source. Since any practical, workable material has magnetic effects at least on the order of diamagnetism, it seemed important to either, a) quantify the magnetic field in addition to the gravity measurement and calibrate the magnetic effects, or, b) design a device which is insensitive to magnetic fields. The latter option was chosen during prototype development. Since it was considered somewhat advantageous for the sensor to be completely non-metallic, this became a design criteria [6].

It was envisioned that it might be possible to begin with a known diamagnetic material and treat it with a paramagnetic compound in order to null the forces which developed in a magnetic field. Ultimately, a test mass of ordinary boro-silicate glass was used. After incorporation into the accelerometer, the mass was treated with a dilute solution of  $FeCl_2$  until the output was nulled at an arbitrary value of the applied field.



## PROTOTYPE FABRICATION

Figure 2 shows a schematic diagram of the TSA. F-SV single-mode fiber was used for the fiber lead and spring segment. The protective housing was fabricated from lucite and quartz tubing. A high magnification was achieved by using a 2 mm spherical ball lens to image the fiber tip.

Some empirical measurements were made to determine the elastic modulus of the fiber, optical magnification, and deflection range prior to the final design. The magnification was measured by translating the lens in a transverse direction using a micropositioner and measuring the deflection at the viewing plane. It was determined that the fiber displacement is limited to 0.36 mm before comatic aberration impairs image visibility. Within this range, the optical and mechanical systems were highly linear. By dividing the rated spot resolution by the viewing plane range, it was determined that the image position resolution was 0.105% full scale deflection: a design relation used to balance the overall range with the sensitivity limit.

The sensor for the advanced prototype was fabricated in a 16-step procedure involving fiber shaping, alignment/assembly procedures, and magnetic nulling. The design data and specifications are given in Appendix 1.

## CALIBRATION

The prototype was calibrated by performing two measurements before encapsulation: a static deflection test to determine the effective spring constant, and a dynamic test to determine the effective mass. These quantities were put into Eq. (8) to determine the responsivity.

In particular, the effective spring constant was computed from the relation,

$$k_{eff} = \frac{g \delta m}{\delta y'} M \quad (11)$$

by placing a 0.1 mm sphere having a mass of approximately 0.1 mg onto the test mass and measuring the deflection at the viewing plane.

Since there is very little damping of the intrinsic sensor, the resonant frequency,  $f$ , is given by,

$$f = \frac{1}{2\pi} \sqrt{\frac{k_{eff}}{m_{eff}}} \quad (12)$$

The period of oscillation was measured, which in conjunction with the effective spring constant determined the effective mass. Calibration data and the determined specifications are found in Appendix 2.

## MAGNETIC EFFECTS

Data were taken for the magnetic response of the test mass while suspended in the accelerometer arrangement. A small solenoid was calibrated and used to purposely apply a field with a high gradient. The graph included as Fig. 3 shows the deflection of the image at the viewing plane as a function of DC voltage applied to the electromagnet. The two plots correspond to the untreated glass test mass, and the mass after uniform treatment with FeCl<sub>2</sub>. Iron chloride and glass were the only materials tried, since optimization of these parameters was beyond the scope of the contractual period. The results which were obtained, although not linear, do show a dramatic reduction in the magnetic response.

For comparison with these empirical results, the magnetic force was calculated by starting with the force density,

$$\frac{d\vec{F}}{dV} = \nabla \vec{M} \cdot \vec{B} \quad (13)$$

where  $\mathbf{F}$  is the force,  $V$  is the volume,  $\mathbf{M}$  is the magnetic moment density, and  $\mathbf{B}$  is the magnetic field.

Assuming a linear, scalar magnetic susceptibility,  $\chi$ , and approximating the magnetic permeability,  $\mu = \mu_0$ , then,

$$\vec{M} = \frac{1}{\mu_0} \chi \vec{B} \quad (14)$$

Integrating over the volume of the material object,

$$F = \frac{2}{\mu_0} \int \chi B \nabla B dV \quad (15)$$

Equation (15) shows that the force intrinsically depends on the product of the field value and field gradient.

A Hall probe was used to calibrate the solenoid. The plot shown in Fig. 4 shows the result of varying the voltage when the probe was placed at a fixed distance of 1 mm from the solenoid. Figure 5, on the other hand, shows the result of varying the distance for a fixed voltage.

The curve  $1.13B(v)e^{-\alpha d}$  was fit to the axial field data, where  $B(v)$  is plotted in Fig. 4. By approximating only an  $x$  coordinate field dependence and integrating over the test mass volume, the force becomes,

$$F = \frac{1.13}{\mu_0} B(v)^2 \chi L H (e^{-2\alpha x_2} - e^{-2\alpha x_1}) \quad (16)$$

This expression was evaluated for untreated glass at  $B = 2100$  Gauss, with  $\chi(\text{glass}) = -1.36 \times 10^{-5}$ ,  $\alpha = 0.1429$ , and the physical dimensions,  $L$  (length),  $H$  (height) and  $W$  (width) =  $x_2 - x_1$ , given in Appendix 1. During the TSA experiment, the solenoid was  $\sim 0.5$  mm from the mass. The calculated force was equivalent to 3.89 mG's, compared to 2.2 mG predicted by Fig. 3 at 50 v.

## CONCLUSIONS

A prototype accelerometer was designed, fabricated and demonstrated having a spatial resolution of a fraction of a cubic centimeter and a rated sensitivity of 25  $\mu\text{G}$  measurement. Magnetic tests provided some illumination on the fundamental level of sensitivity of such devices.

The TSA has the ability to produce a directly observable output, or can be used in conjunction with a fiber-optic image preserving cable routed to a CCD camera. The typical vibration response on an optics isolated steel table is in the range, 100 to 800  $\mu\text{G}$ 's. This is largely due to the fact that no damping was provided intrinsically to the sensor due to buoyancy and fabrication considerations. However, image analysis done by computer can allow a variable time constant in order to reduce vibrational fluctuations down below the sensitivity limit.

The developmental work done toward this project inspired several ideas for simultaneous vector measurement of magnetic and gravitational fields at the same spatial location. Additionally, it was conjectured that an alternative approach to quantifying gravitational effects of superconductors may be possible by considering the magnetogravitational component. These fields resulting from electromagnetic interactions in superconductors may be many orders of magnitude larger than are ordinarily producible, and may be detectable by a new type of optical sensor for which feasibility investigations have begun.

## REFERENCES

1. Podkletnov, E.E., Nieminen, R., "A possibility of gravitational force shielding by bulk  $\text{YBa}_2\text{Cu}_3\text{O}_{7-x}$  superconductor," *Physica C*, 203, (1992), p. 441.
2. Noever, D., private communication, September 1997.
3. Podkletnov, E.E., Levit, A.D., "Gravitation shielding properties of composite bulk  $\text{YBa}_2\text{Cu}_3\text{O}_{7-x}$  superconductor below 70 K under electro-magnetic field," in press.
4. Torr, D.G., Li, N., "Gravitoelectric-electric coupling via superconductivity," *Phys. Lett.* 6 (1993), p. 371.

5. Modanese, G., "Theoretical analysis of a reported weak gravitational shielding effect," in press.
6. Li, N., private communications, August 1997.

## **ACKNOWLEDGEMENTS**

The authors would like to thank their project managers, Mr. Ron Koczor (NASA/MSFC) and Mr. Whitt Brantley (NASA/MSFC), for providing the opportunity to conduct the research; project scientists Dr. David Noever (NASA/MSFC) and Dr. Ning Li (UAH/CMDS) for assisting with the technical development of the TSA; and, Dr. John Dimmock (UAH/Director, CAO) and Dr. Charles Lundquist (UAH/Director, CMDS) for reviewing and commenting on the work.

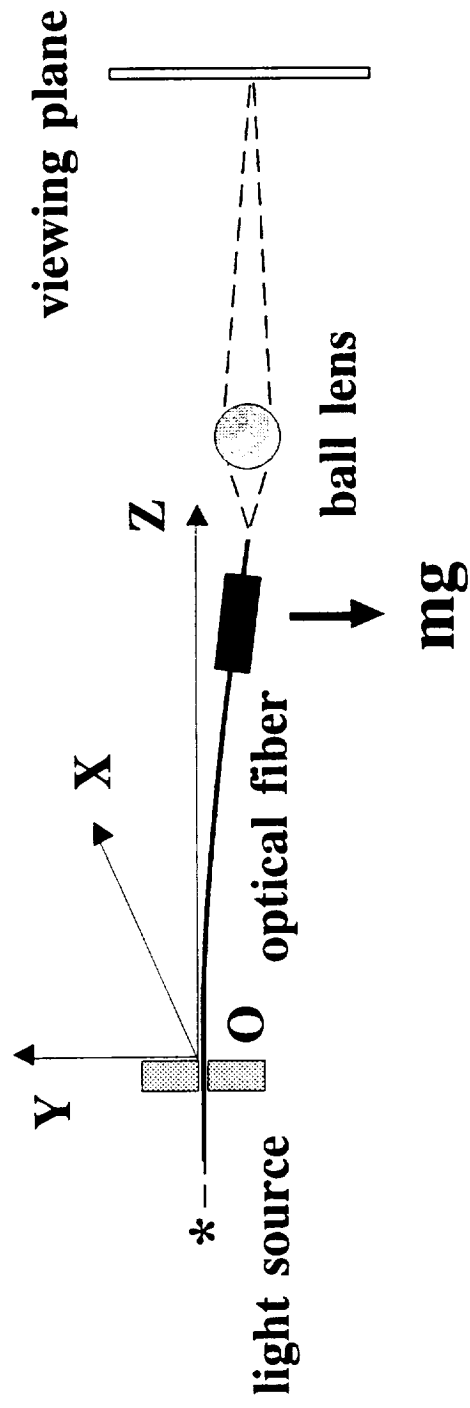


**Figure 1.** Schematic diagram of the measurement system.

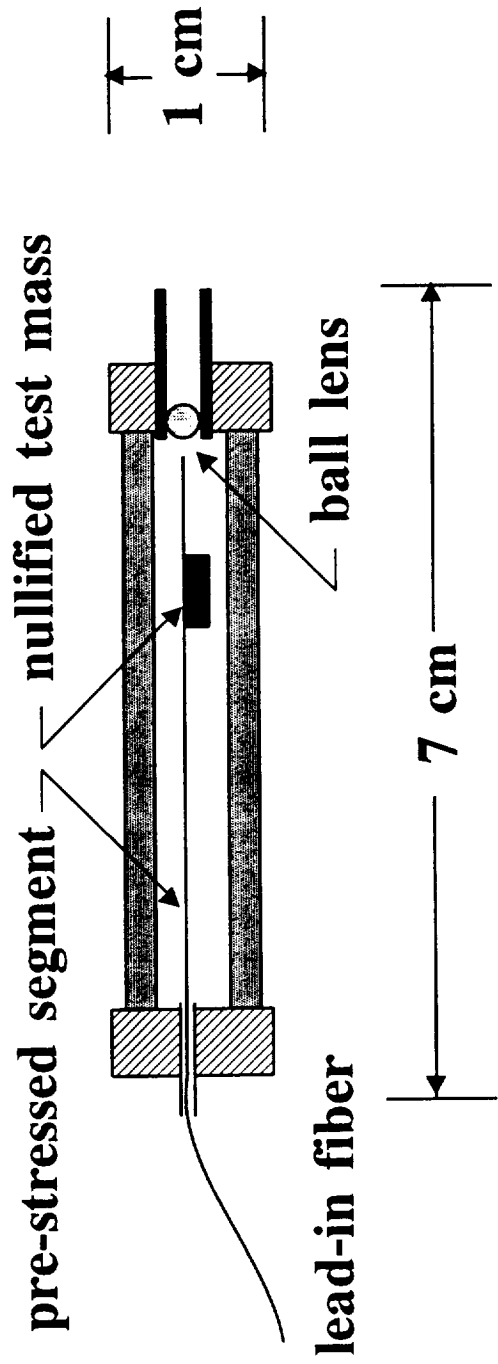


**Figure 2.** The Transversely Suspended Accelerometer (TSA).

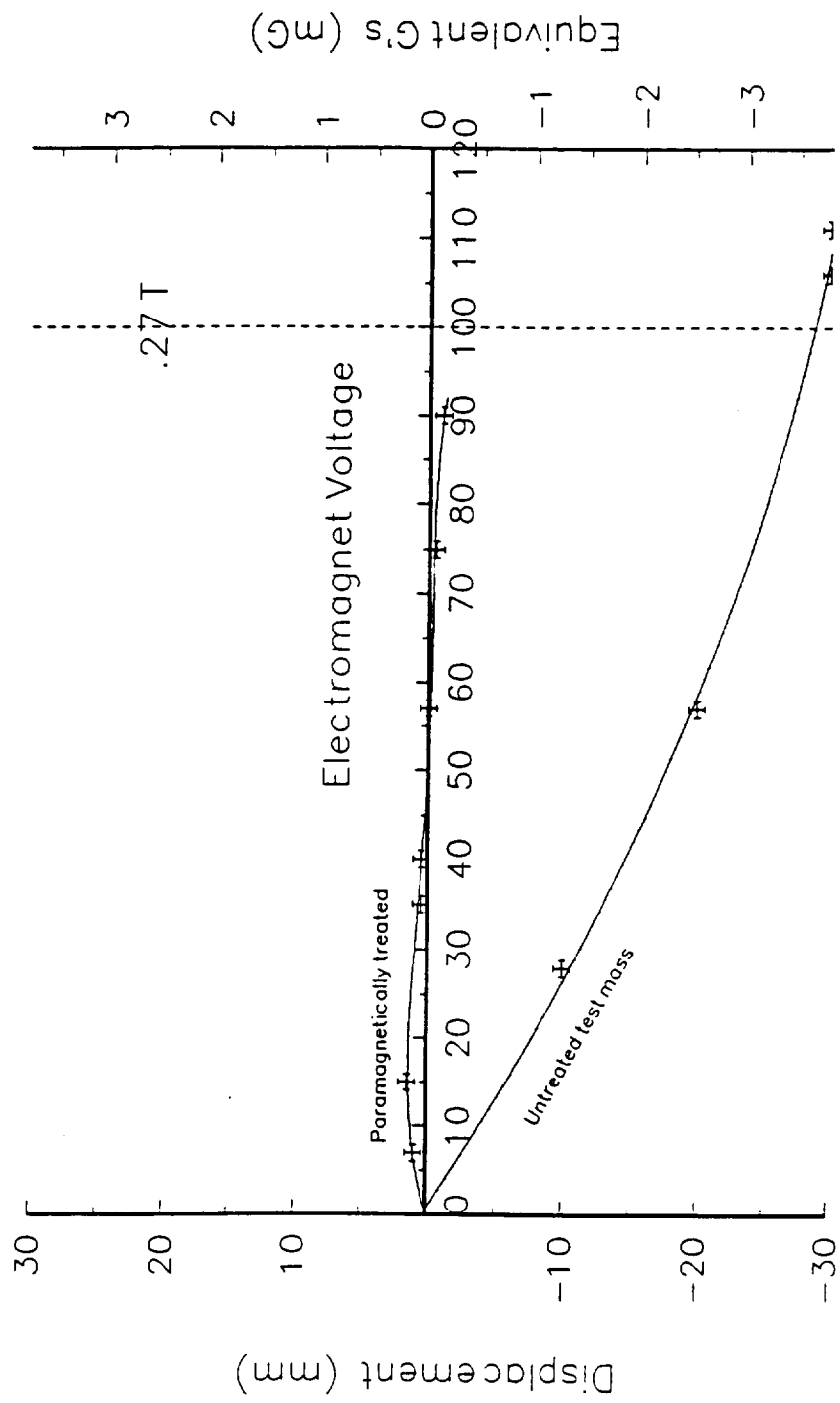


**Figure 3.** Magnetic response of the TSA.

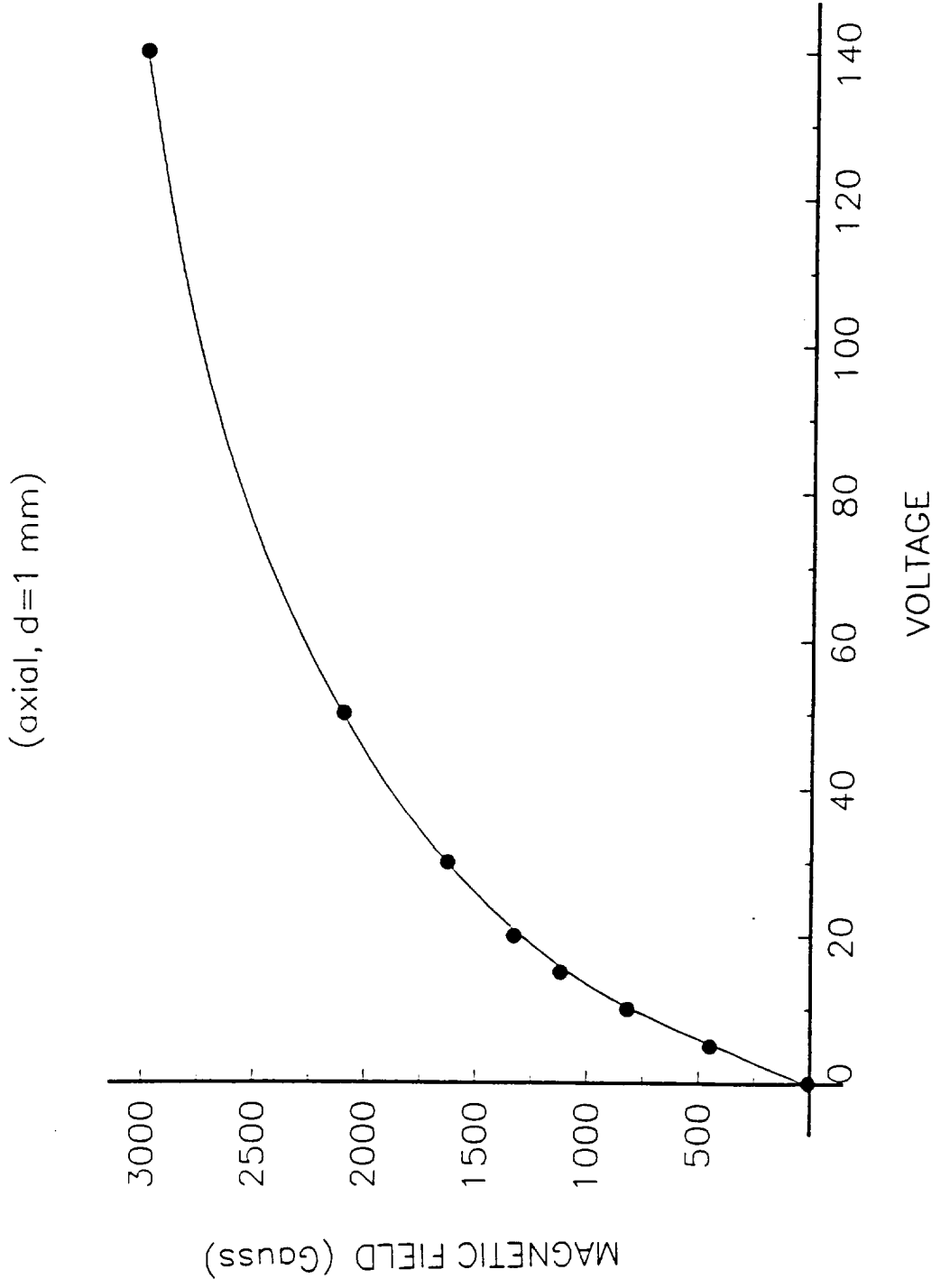


**Figure 4.** Small solenoid calibration: magnetic field versus voltage.



(B(v)=1100 G)

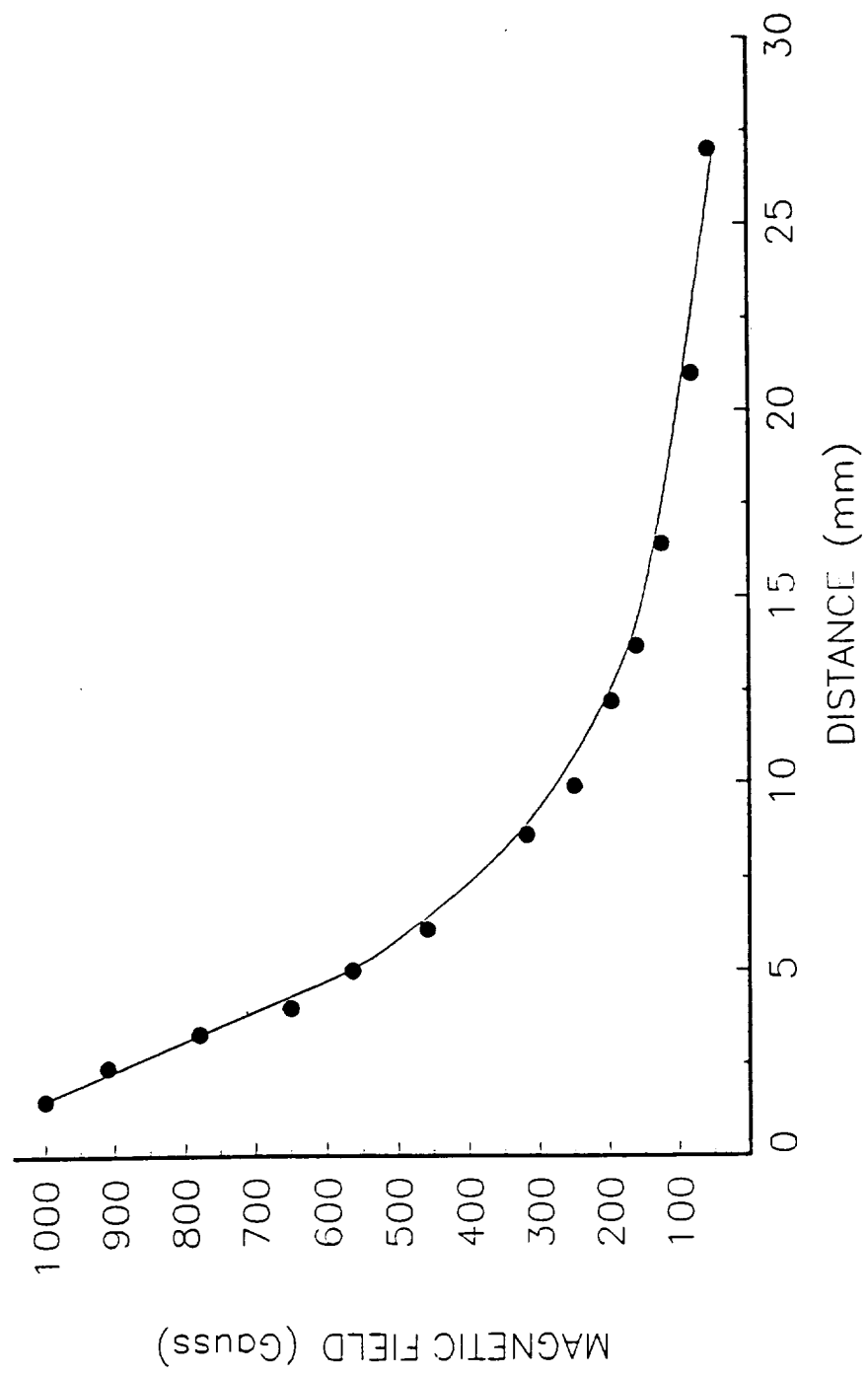


**Figure 5.** Small solenoid calibration: axial field dependence.

## APPENDIX 1. SENSOR DESIGN DATA

### Fiber

Type:	F-SV single-mode
Core diameter:	4 $\mu\text{m}$
Cladding diameter:	125 $\mu\text{m}$
Elastic modulus:	$6.8 \times 10^{10}$ Pa

### Lens

Diameter:	2 mm
Effective aperture:	0.36 mm
Back focal length:	1.1 mm

### Design of TSA

$\delta G$ (full scale):	20 mG's
Resolution:	0.105% full scale = 25 $\mu\text{G}$ 's
$m^3$ (from Eq. (6)):	$4.5 \times 10^{-9}$ (mks units)
For $m \sim 70$ mg:	$l \sim 3.6$ cm (see footnote) <sup>2</sup>
Initial deflection:	18 mm
Prestress curve:	$y = 2 \times 10^{-4} (105 - z) z^2$ for $z < 36$ (in mm)

### Measured fabrication parameters

Fiber length (end to c.m.):	3.66 cm
Length $b$ (mass to fiber tip):	1.10 cm
Test mass dimensions:	$L = 4.9$ mm, $W = 3.6$ mm, $H = 2.0$ mm
Magnification at 1 m view:	876
Spot size at 1.3 m (FW $\sim 95\%$ ):	0.9 mm (see footnote) <sup>3</sup>

---

<sup>2</sup> As tabulated in the measured fabrication parameters, the effective length ended up larger with a smaller effective mass.

<sup>3</sup> The theoretical spot size at a distance of 1.3 m was 1.0 mm.

## APPENDIX 2. SENSOR CALIBRATION DATA AND SPECIFICATIONS

### Static procedure

Microsphere mass:	~ 0.1 mg
Average displacement for microsphere addition:	1.60 cm (@ 1.3 m view)
$k_{\text{eff}}$ from $\delta F/(\delta y'/M)$ :	0.0537 N/m
$k_{\text{eff}}$ calculated, Eq. (5):	0.0499 N/m

### Dynamic procedure

Average time per oscillation:	0.1912 s
Resonant frequency:	5.230 Hz
Effective mass, Eq. (12):	46.3 mg

### Responsivity @ 1 m

From Eq. (8):	164 $\mu\text{G}/\text{mm}$
---------------	-----------------------------

### Rated readability @ 1 m

Spot size x 0.2 = 0.16 mm:	=> 25 $\mu\text{G}$
----------------------------	---------------------